

## Supporting information

### Various States of Water Species in an Anion Exchange Membrane Characterized by Raman Spectroscopy under Controlled Temperature and Humidity

Solomon Wekesa Wakolo,<sup>a</sup> Donald A. Tryk,<sup>b</sup> Hiromichi Nishiyama,<sup>b,#</sup> Kenji Miyatake,<sup>b,d,d</sup> Akihiro Iiyama,<sup>b</sup> Junji Inukai<sup>b,c</sup>

<sup>a</sup>Integrated Graduate School of Medicine, Engineering, and Agricultural Sciences, University of Yamanashi, 4-3-37 Takeda, Kofu, Yamanashi 400-8510, Japan

<sup>b</sup>Hydrogen and Fuel Cell Nanomaterials Research Center, University of Yamanashi, 6-43 Miyamae, Kofu, Yamanashi 400-0021, Japan

<sup>c</sup>Clean Energy Research Center, University of Yamanashi, 4-3-11 Takeda, Kofu, Yamanashi 400-8510, Japan

<sup>d</sup>Department of Applied Chemistry, Waseda University, Tokyo 169-8555, Japan

<sup>#</sup>Present address: LIB Technical Center, GS Yuasa International Ltd., 780-1, Hachiya, Ritto, Shiga 520-3021, Japan

## Table of Contents

### 1. Supporting Experimental Results

Figure S1. 1.0 M NaOH spectrum deconvoluted into seven Gaussian bands

Figure S2. 16.0 M NaOH spectrum deconvoluted into seven Gaussian bands

Figure S3. Change in the area under each of the five deconvoluted OH sub bands within the OH band of NaOH with changing molar concentration.

Figure S4. Water uptake in QPAF4 with RH

Figure S5. Raman spectrum calibration Graph

Figure S6. Spectra of de-hydrated QPAF-4 membrane.

### 2. Density Functional Theory

#### a. Methods

Figure S7. Final optimized structure of QPAF-4 fragment

#### b. Results

Figure S8. Simulated Raman spectra

## 1. Supporting Experimental Results

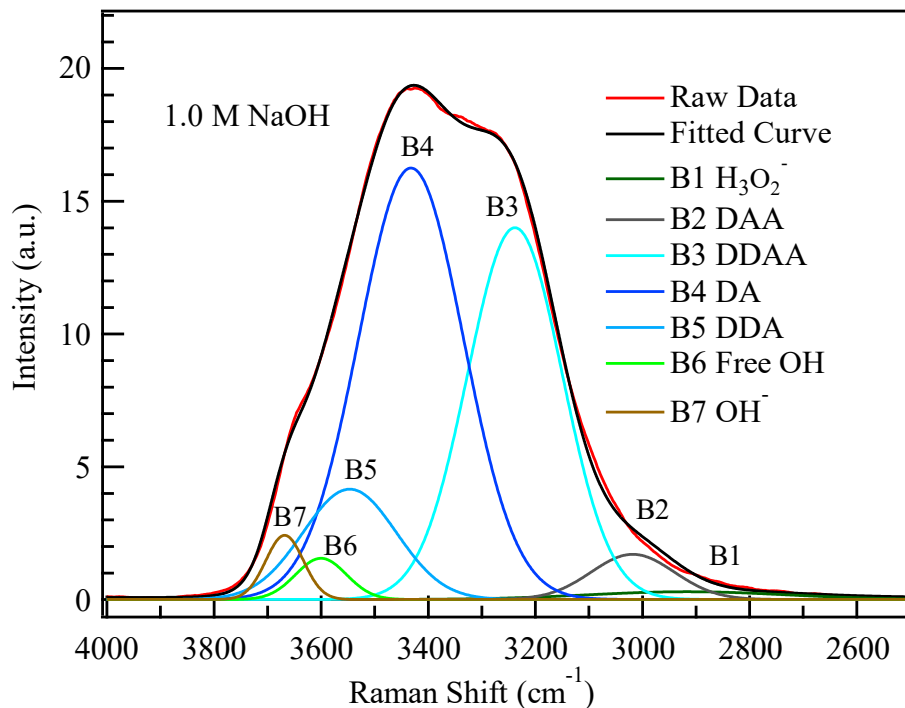


Figure S1. Spectrum in 1.0 M NaOH deconvoluted into seven Gaussian bands.

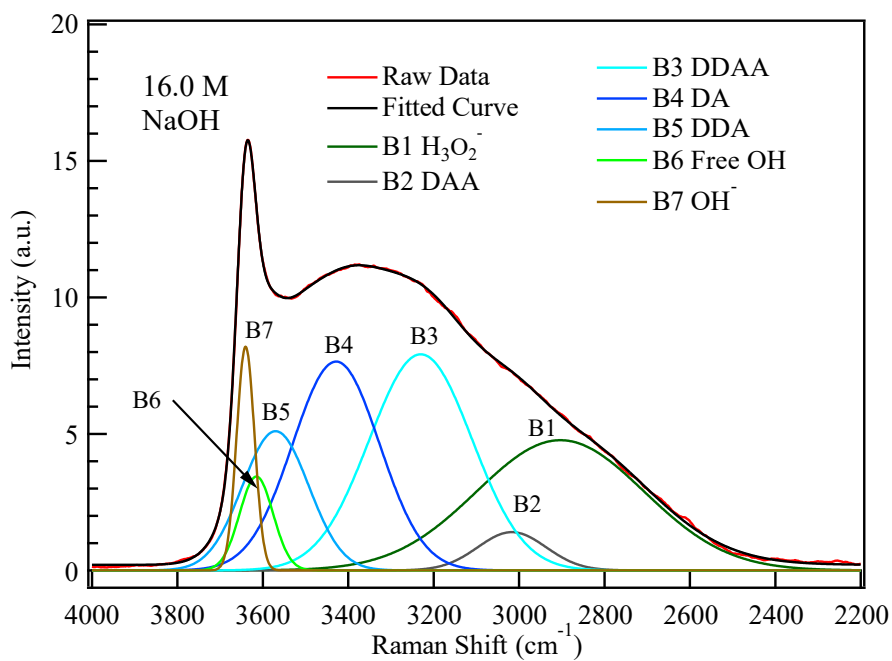


Figure S2. Spectrum in 16.0 M NaOH deconvoluted into seven Gaussian bands.

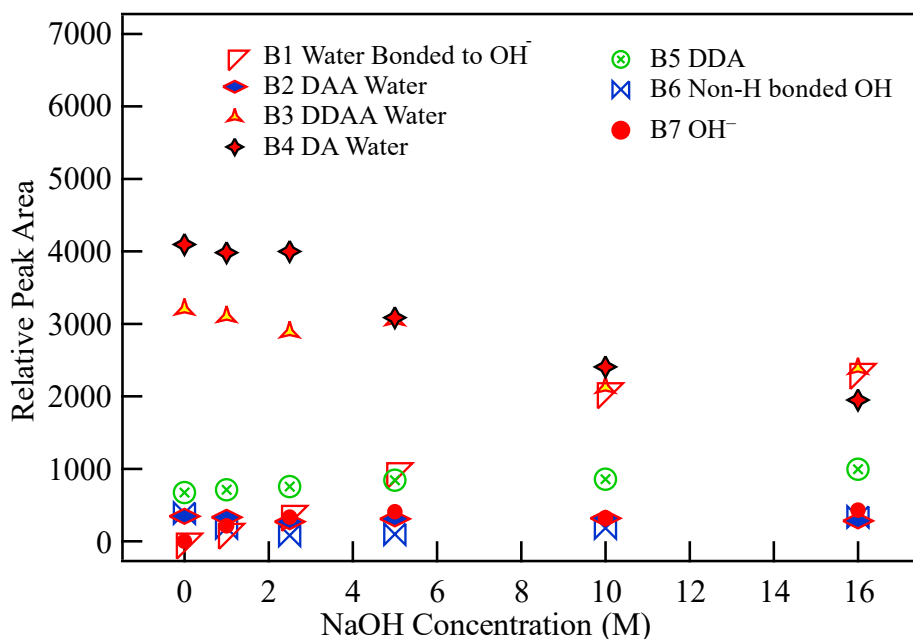


Figure S3. The areas of the five deconvoluted OH sub-bands of the OH stretching band of NaOH with molar concentration. The 0 M concentration points refer to the spectrum of pure water.

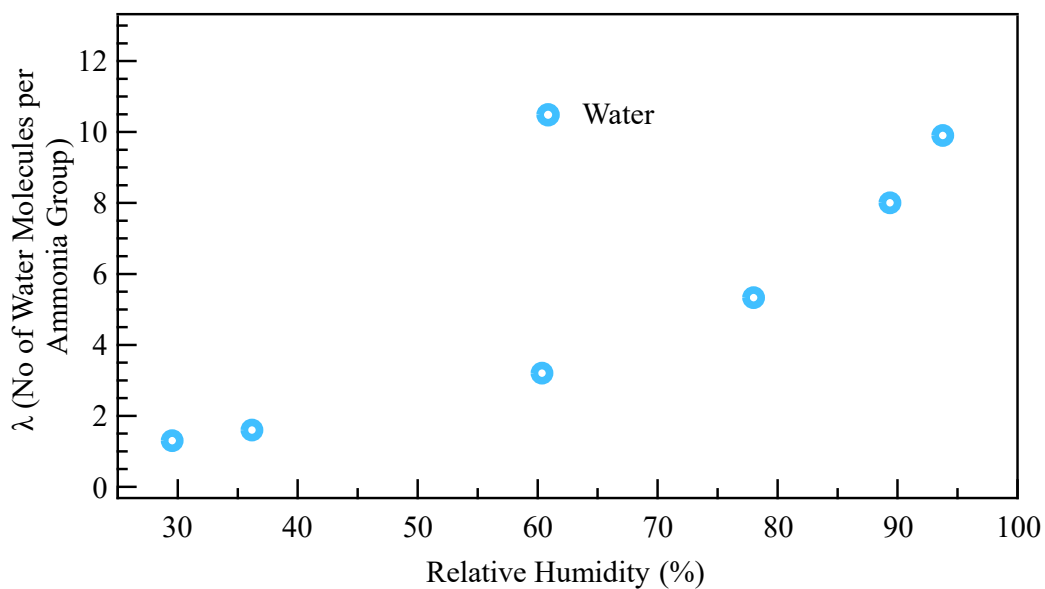


Figure S4. Water uptake in QPAF-4 with RH.

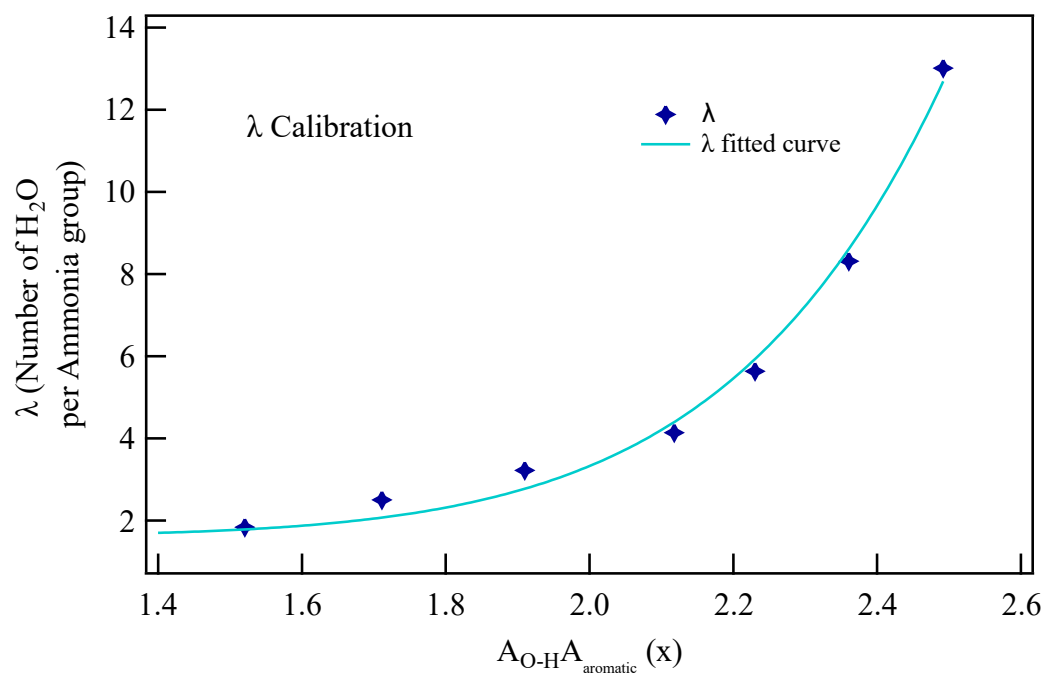


Figure S5. Raman spectrum calibration curve. The relationship between  $\lambda$  and the area ratio  $A_{\text{OH}}/A_{\text{aromatic}} (x)$  is given by  $\lambda=1.6148+0.0047297x^{8.4969}$ .

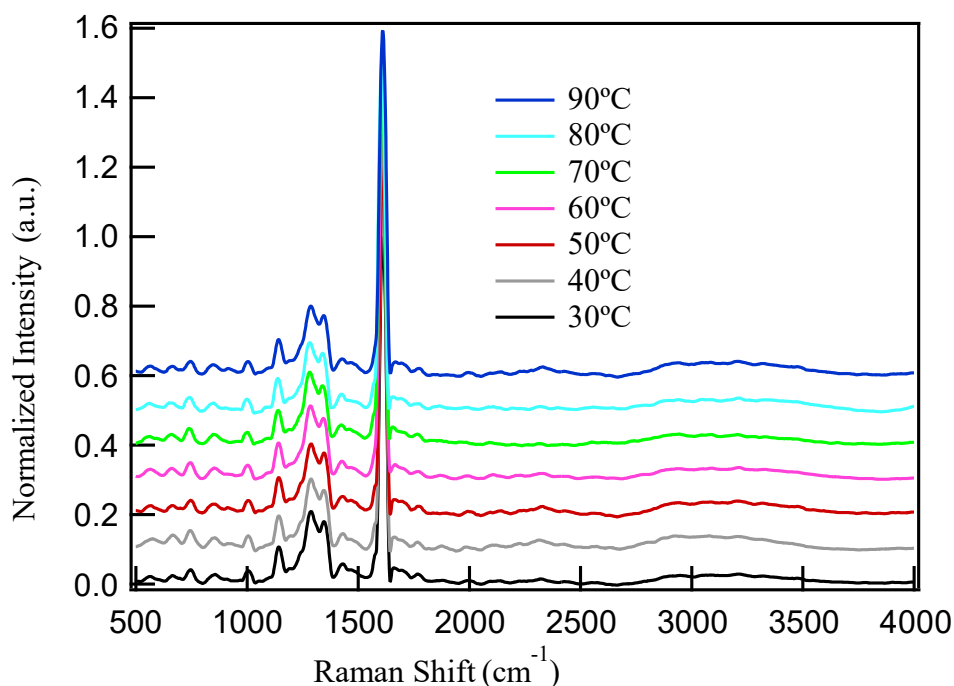


Figure S6. The spectra of de-hydrated QPAF-4 membrane on silicon substrate at different temperatures.

## 2. Density Functional Theory

### a. Methods

A representative section of the QPAF-4 structure that included both hydrophobic and hydrophilic moieties was used for the density functional theory (DFT) calculations. The hydrophilic moiety included two tetraalkylammonium groups, each with an associated hydroxide anion, and 20 water molecules were randomly placed to surround these functional groups and provide a hydrogen-bonded network between them (Figure S6). First, this structure was subjected to a molecular dynamics (MD) calculation in order to obtain a realistic arrangement of the water molecules. Then, two stages of geometry optimisation were carried out, first with medium quality and second with fine quality, as described below in more detail. The final optimised structure was then subjected to vibrational analysis of both  $\text{OH}^-$  anions, the 20 water molecules, and representative parts of the ionomer itself. The vibrational frequencies of the various O-H contributions were finally used to generate a spectrum.

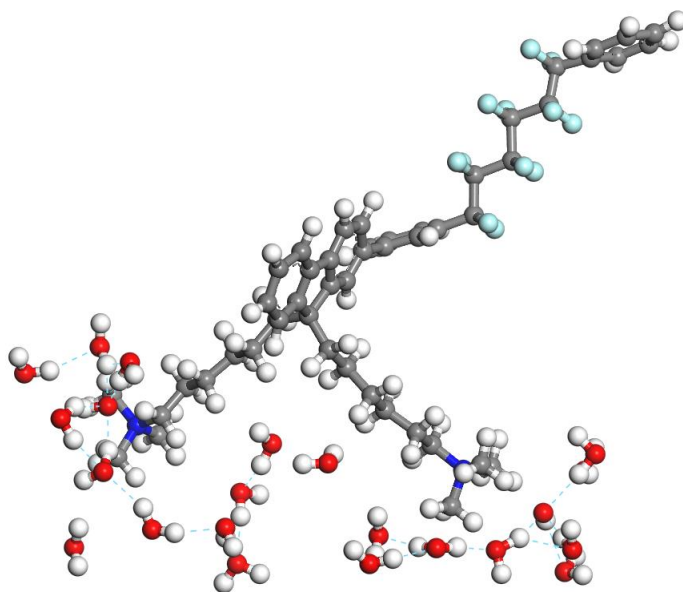


Figure S7. Final optimized structure of QPAF-4 fragment including both hydrophobic and hydrophilic moieties, the latter including two tetraalkylammonium cations, plus two OH<sup>-</sup> and 20 water molecules. Colour scheme: carbon (grey), hydrogen (white), fluorine (light blue), oxygen (red).

The DMol<sup>3</sup> DFT application was used as part of the BIOVIA Materials Studio, v. 2021 (Dassault Systeme) platform<sup>1,2</sup>. The initial ab initio MD calculation was carried out with the hardness-conserving semilocal pseudopotential (dspp)<sup>3</sup> with the PBE functional<sup>4</sup>. The simple Nosé-Hoover thermostat for 200 fs at 300 K was used<sup>5,6</sup>. The final configuration of the MD calculation was then subjected to geometry optimisation, first with medium settings ( $2 \times 10^{-5}$  Ha energy convergence,  $4 \times 10^{-3}$  Å gradient convergence, displacement convergence  $5 \times 10^{-3}$  Å, scf density convergence  $1 \times 10^{-5}$  Ha), and then with fine settings ( $1 \times 10^{-5}$  Ha energy convergence,  $2 \times 10^{-3}$  Å gradient convergence, displacement convergence  $5 \times 10^{-3}$  Å, scf density convergence  $1 \times 10^{-6}$  Ha). Both were all-electron calculations and used the v. 4.4 basis file. The vibrational frequencies were also carried out with fine settings. To generate the spectrum, the individual bands were subjected to Gaussian broadening factors of  $1 \text{ cm}^{-1}$  (minimal broadening) and  $200 \text{ cm}^{-1}$  (realistic broadening).

#### b. Results

The calculated Raman spectrum contains some of the features of the experimental spectrum but overemphasises the high wavenumber region. The main reasons for this are (a) all of the bands have been given equal intensity in the calculation, whereas it is well known that the intensity should decrease with increasing wavenumber of O-H stretching

as the degree of hydrogen bonding decreases; and (b) in the calculation, there would be a disproportionate number of free OH groups, i.e., those with essentially zero H-bonding, with resulting frequencies in the 3700-3800  $\text{cm}^{-1}$  region. There are several predicted vibrations in the low-wavenumber region that are due to water OH groups that are H-bonded to hydroxide oxygen. As explained in the main text, although these bands might be observed experimentally, they are difficult to distinguish from interference features.

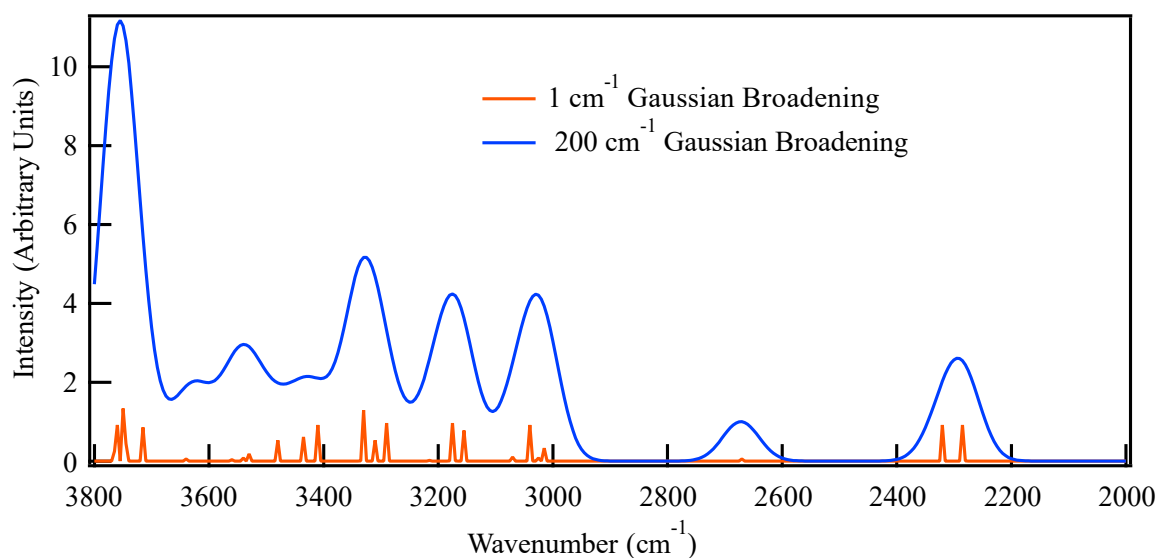


Figure S8. Simulated Raman spectra with 1  $\text{cm}^{-1}$  (orange) and 200  $\text{cm}^{-1}$  (blue) levels of Gaussian broadening.

## References

- 1 B. Delley, An all-electron numerical method for solving the local density functional for polyatomic molecules, *J. Chem. Phys.*, 1990, **92**, 508–517.
- 2 B. Delley, From molecules to solids with the DMol3 approach, *J. Chem. Phys.*, 2000, **113**, 7756–7764.
- 3 B. Delley, Hardness conserving semilocal pseudopotentials, *Phys. Rev. B - Condens. Matter Mater. Phys.*, 2002, **66**, 1–9.
- 4 J. P. Perdew, K. Burke and M. Ernzerhof, Erratum: Generalized gradient approximation made simple (Physical Review Letters (1996) 77 (3865)), *Phys. Rev. Lett.*, 1997, **78**, 1396.
- 5 S. Nosé, A unified formulation of the constant temperature molecular dynamics methods, *J. Chem. Phys.*, 1984, **81**, 511–519.
- 6 Y. Kassir, M. Kupiec, A. Shalom and G. Simchen, Canonical dynamics: Equilibrium phase-space distributions, *Phys. Rev. A*, 1985, **9**, 1695–1697.